Hindawi
Shock and Vibration
Volume 2018, Article ID 1538936, 17 pages
https://doi.org/10.1155/2018/1538936

Research Article

Generalized-Disturbance Rejection Control for Vibration Suppression of Piezoelectric Laminated Flexible Structures

Xiao-Yu Zhang[1], **Run-Xiao Wang**[1], **Shun-Qi Zhang**[2], **Zhan-Xi Wang**[1], **Xian-Sheng Qin**[1] **and Rüdiger Schmidt**[3]

[1] *School of Mechanical Engineering, Northwestern Polytechnical University, West Youyi Street 127, Xi'an 710072, China*
[2] *School of Mechatronic Engineering and Automation, Shanghai University, Shangda Road 99, Shanghai 200444, China*
[3] *Institute of Structural Mechanics and Lightweight Design, RWTH Aachen University, Wüllnerstraße 7, 52062 Aachen, Germany*

Correspondence should be addressed to Shun-Qi Zhang; sqzhangnpu@hotmail.com

Received 25 September 2017; Revised 27 December 2017; Accepted 9 January 2018; Published 19 February 2018

Academic Editor: Francesco Ripamonti

In the framework of disturbance rejection (DR) control, the paper proposes a generalized-disturbance rejection (GDR) control with proportional-integral (PI) observer for vibration suppression of smart structures under any unknown continuous disturbances. In the proposed GDR-PI control, a refined state space model is first constructed, and a generalized disturbance including the disturbance influence matrices, unknown physical disturbances, and state variables is defined. In the closed loop of GDR-PI control, physical disturbances can be counteracted indirectly by feeding back estimated generalized disturbances. By this means, the GDR-PI control remedies most of the defects in conventional DR control and has excellent performances especially in the following situations: (i) the disturbances are completely unknown; (ii) the number of sensor signals is less than the number of disturbances; (iii) the unknown disturbances vary fast. Finally, the GDR-PI control is validated and compared with H_∞ state feedback control and conventional DR control available in the literature for vibration suppression of smart beams.

1. Introduction

Flexible structures are widely used in the field of aerospace engineering because of light weight, which however are very sensitive to vibrations because of their low stiffness and damping ratios. The unwanted vibrations not only degrade the mechanical performance of structures but sometimes also cause destructive results, for example, flutter problems of flight vehicles [1], vibrations of flexible space antenna [2], and manipulator [3]. To break the contradiction between light weight and structural stability, smart structures were proposed and developed increasingly by many researchers for vibration suppression, in which smart materials, for example, piezoelectric, magnetostrictive materials and shape memory alloys, are tightly integrated. As can be seen, most of those unwanted vibrations are usually caused by unknown external or internal disturbances, which make the system unstable and hard to control. Therefore, a proper control strategy plays a very important role in the case of smart structures under unknown disturbances.

During the past few decades, many control methods have been proposed and developed for vibration suppression of smart structures, including classical control theory, modern control theory, and intelligent control theory. Among them, negative velocity feedback control [3–9] and positive position feedback control [10–14] became the two most popular classical control strategies for easy implementation. As the most famous control method in industry, PID control was applied to vibration suppression in many papers [15–19]. Another classical control strategy is so-called bang-bang control, which can be found in, for example, [20–23] among many others. In the field of modern control theory, Linear Quadratic Regulator (LQR) control and Linear Quadratic Gaussian (LQG) control are the two most popular choices for vibration suppression, which can be found in [24–27] and [25, 28–33], respectively. Furthermore, applications of

Lyapunov control [24, 34–36] were also conducted by many researchers. Some advanced control methods for smart structures came into vogue in recent years. For example, sliding model control [37–39] and model predictive control [40–42] were implemented in many researches of vibration suppression of smart structures. In the aspect of artificial intelligence algorithms, controllers for vibration suppression of smart structures are developed using online self-organizing fuzzy logic control [43], multiobjective differential evolution algorithm optimized fuzzy logic control [44], and hybrid algorithm combining fuzzy logic and proportional-integral control [45]. Moreover, neural network control was applied to smart structures numerically [46–48] and experimentally [49–51].

However, the above-mentioned control strategies did not take into account the unknown disturbances. Since many unwanted vibrations are caused by unknown disturbances, especially the continuous and strong ones, it is not hard to see that vibrations will be extremely suppressed if the unknown disturbances are considered during the controller design process. There are only a few control methods considering the influence of disturbances or aiming at rejecting disturbances, for example, H_∞ control, adaptive control, and disturbance rejection control. A considerable amount of literatures can be found on H_∞ robust control [52–54] and adaptive control [55–58] for vibration suppression problems. Nevertheless, the disturbances considered in H_∞ controllers are normally measurement noises with low amplitude and zero mean value. In contrast, the disturbances that cause vibrations are much stronger than measurement noises, which makes it difficult to be attenuated efficiently using H_∞ control. On the other hand, although disturbance rejection can be achieved by adaptive regulation in some situations, the adaptive control is hindered from wide applications by deficiencies like complexity, narrow band constraint, or water bed effect. In a more efficient way, disturbance rejection (DR) control presents a mechanism in which disturbances are counteracted by feeding the estimated disturbances back to the system, leading to excellent disturbance rejecting performance and great advantage in suppressing vibrations caused by unknown disturbances.

Because of the excellent disturbance rejecting performance and easy implementation, DR control has attracted the interest of many researchers. In the framework of DR control, Han [59] and Gao [60] developed an active disturbance rejection control (ADRC) for single-input single-output systems. Based on acceleration compensation, Li et al. [61, 62] applied ADRC to piezoelectric multimode vibration control for stiffened plate with chaos optimization method and Smith Predictor technology, which were both verified experimentally. On the other hand, Müller and Lückel [63] proposed and developed a DR control with proportional-integral (PI) observer for multi-input multioutput systems. Disturbances with low frequencies can be estimated and counteracted in the DR-PI control. Later, the PI observer was extended to a generalized proportional-integral (GPI) observer by Zhang et al. [64, 65] for vibration suppression of smart structures, which is able to estimate disturbances with high frequencies. The GPI observer utilizes a combination of constant terms and sine (or cosine) functions as the fictitious disturbance model, which results in precise estimation of disturbances with frequencies roughly known. Vibrations of smart structures excited by periodic disturbances with low- or high-order frequencies can be successfully suppressed by the DR-GPI control.

However, the performances of DR-PI control and DR-GPI control may deteriorate when some requirements on sensor signals and disturbance information cannot be satisfied. For example, in DR control, it is required that the disturbance influence matrices must be known and the number of sensor signals cannot be less than that of disturbances. Moreover, the DR-PI control is only valid for disturbances varying very slow. Although the DR-GPI control can be applied for periodic disturbances with high-order frequencies, the frequencies must be known or roughly known. In order to remedy the aforementioned shortcomings, based on the work of Zhang et al. [64, 65], this paper proposes a refined disturbance rejection control method, named as generalized-disturbance rejection (GDR) control, for vibration suppression of smart structures under any unknown continuous disturbances. In the proposed GDR control, a refined state space model is first constructed, in which a generalized disturbance is defined including the disturbance influence matrices, unknown disturbances, and state variables. In such a way, using either the PI or GPI observer, the generalized disturbances can be estimated and fed back to the controller. Unlike the conventional DR control, the proposed method cannot estimate the real disturbances but rather the generalized disturbances with the information of disturbances and state variables. Therefore, the GDR control remedies most of the shortcomings in conventional DR control and has excellent performances in situations as, but not limited to, the following: (i) the disturbance influence matrices are unknown; (ii) the number of sensor signals is less than the number of disturbances; (iii) the disturbances are periodic ones with unknown high-order frequencies or random ones varying fast. Finally, the GDR-PI control is validated and compared numerically with H_∞ state feedback control and DR-GPI control for vibration suppression of a piezoelectric laminated flexible smart beam. Results show that the GDR-PI control achieves better vibration suppression performance in the situations mentioned above.

2. System Modeling

2.1. Dynamic Model. To design and validate a controller for vibration suppression, a mathematical dynamic model of a piezoelectric laminated smart structure is needed. Using the finite element (FE) method based on the First-Order Shear Deformation (FOSD) hypothesis, the dynamic FE model is obtained as [66–69]

$$\mathbf{M}_{uu}\ddot{\mathbf{q}} + \mathbf{C}_{uu}\dot{\mathbf{q}} + \mathbf{K}_{uu}\mathbf{q} + \mathbf{K}_{u\phi}\boldsymbol{\phi}_a = \mathbf{f}_f, \tag{1}$$

$$\mathbf{K}_{\phi u}\mathbf{q} + \mathbf{K}_{\phi\phi}\boldsymbol{\phi}_s = \mathbf{0}. \tag{2}$$

In (1), $\mathbf{M}_{uu}$, $\mathbf{C}_{uu}$, $\mathbf{K}_{uu}$, $\mathbf{K}_{u\phi}$, $\mathbf{q}$, $\boldsymbol{\phi}_a$, and $\mathbf{f}_f$ denote the mass matrix, the damping matrix, the stiffness matrix, the piezoelectric coupled stiffness matrix, the nodal displacement

vector, the actuation voltage vector, and the external force vector, respectively. In (2), $\mathbf{K}_{\phi u}$, $\mathbf{K}_{\phi\phi}$, and $\boldsymbol{\phi}_s$ represent the coupled capacity matrix, the piezoelectric capacity matrix, and the sensor voltage vector, respectively.

2.2. State Space Model. For controller design convenience, a state space model is derived from the dynamic FE model given in (1) and (2) as

$$\dot{\mathbf{x}}(t) = \mathbf{A}\mathbf{x} + \mathbf{B}\mathbf{u} + \mathbf{N}\mathbf{f}, \tag{3}$$

$$\mathbf{y}(t) = \mathbf{C}\mathbf{x} \tag{4}$$

in which the state vector $\mathbf{x}$, the control input vector $\mathbf{u}$, and the system output vector $\mathbf{y}$ are, respectively, defined as

$$\begin{aligned} \mathbf{x} &= \begin{Bmatrix} \mathbf{q} \\ \dot{\mathbf{q}} \end{Bmatrix}, \\ \mathbf{u} &= \boldsymbol{\phi}_a, \\ \mathbf{y} &= \boldsymbol{\phi}_s. \end{aligned} \tag{5}$$

Furthermore, vector $\mathbf{f}$ denotes the physical disturbance that can influence the control system of smart structures. Physical disturbance can be any unknown external forces $\mathbf{f}_f$, nonlinearities $\mathbf{f}_n$, system errors $\mathbf{f}_e$, and so forth. Hence the physical disturbance vector $\mathbf{f}$ can be expressed as

$$\mathbf{f} = \begin{Bmatrix} \mathbf{f}_f \\ \mathbf{f}_n \\ \mathbf{f}_e \end{Bmatrix}. \tag{6}$$

Assuming $\mathbf{N}_f$, $\mathbf{N}_n$, and $\mathbf{N}_e$ are the influence matrices of $\mathbf{f}_f$, $\mathbf{f}_n$, and $\mathbf{f}_e$, respectively, the physical disturbance influence matrix $\mathbf{N}$ can be obtained as

$$\mathbf{N} = \begin{bmatrix} \mathbf{N}_f & \mathbf{N}_n & \mathbf{N}_e \end{bmatrix}. \tag{7}$$

For simplicity, external force is considered as the only physical disturbance in this paper, which leads to

$$\begin{aligned} \mathbf{f} &= \mathbf{f}_f, \\ \mathbf{N} &= \mathbf{N}_f. \end{aligned} \tag{8}$$

The system matrix $\mathbf{A}$, the control input matrix $\mathbf{B}$, the external force influence matrix $\mathbf{N}_f$, and the system output matrix $\mathbf{C}$ are calculated by

$$\mathbf{A} = \begin{bmatrix} \mathbf{0} & \mathbf{I} \\ -\mathbf{M}_{uu}^{-1}\mathbf{K}_{uu} & -\mathbf{M}_{uu}^{-1}\mathbf{C}_{uu} \end{bmatrix}, \tag{9}$$

$$\mathbf{B} = \begin{bmatrix} \mathbf{0} \\ -\mathbf{M}_{uu}^{-1}\mathbf{K}_{u\phi} \end{bmatrix}, \tag{10}$$

$$\mathbf{N}_f = \begin{bmatrix} \mathbf{0} \\ \mathbf{M}_{uu}^{-1} \end{bmatrix}, \tag{11}$$

$$\mathbf{C} = \begin{bmatrix} -\mathbf{K}_{\phi\phi}^{-1}\mathbf{K}_{\phi u} & \mathbf{0} \end{bmatrix}. \tag{12}$$

The state space model given in (3) and (4) is named as the original state space model in order to distinguish it from the refined state space model in the later section of GDR control design.

3. Generalized-Disturbance Rejection Control

3.1. Refined State Space Model. In the conventional DR control, accurate disturbance influence matrices are needed for the design of PI or GPI observer so that the disturbances can be estimated. However, the physical disturbance influence matrix $\mathbf{N}$ is assumed as unknown in this paper, which leads to failure in observer design. Therefore, the physical disturbances cannot be estimated directly in the original state space model due to the lack of accurate disturbance influence matrices. As a solution, the generalized disturbance, which includes disturbance influence matrices, unknown disturbances, and state variables, is utilized in the GDR control to achieve indirect estimation and counteraction of physical disturbances with unknown influence matrices. To construct the generalized disturbance, a refined state space model is built first, which is transformed from the original state space model in (3) and (4), by introducing a new state vector as

$$\mathbf{z} = \begin{Bmatrix} \mathbf{z}_1 \\ \mathbf{z}_2 \end{Bmatrix} = \begin{Bmatrix} \mathbf{y} \\ \dot{\mathbf{y}} \end{Bmatrix}. \tag{13}$$

Here, $\mathbf{z}$ is the new state vector composed of $\mathbf{z}_1$ and $\mathbf{z}_2$ which are equal to $\mathbf{y}$ and $\dot{\mathbf{y}}$, respectively. Substituting (4) into (13) and taking the time derivative of (13) one obtains

$$\dot{\mathbf{z}} = \begin{bmatrix} \dot{\mathbf{y}} \\ \mathbf{C}\left(\mathbf{A}\dot{\mathbf{x}} + \mathbf{B}\dot{\mathbf{u}} + \mathbf{N}\dot{\mathbf{f}}\right) \end{bmatrix}. \tag{14}$$

From (10) and (12) it can be easily found out that $\mathbf{CB} = \mathbf{0}$. Substituting (3) and (13) into (14) yields

$$\begin{aligned} \dot{\mathbf{z}} &= \begin{bmatrix} \mathbf{z}_2 \\ \mathbf{CA}(\mathbf{A}\mathbf{x} + \mathbf{B}\mathbf{u} + \mathbf{N}\mathbf{f}) + \mathbf{C}\mathbf{N}\dot{\mathbf{f}} \end{bmatrix} \\ &= \begin{bmatrix} \mathbf{z}_2 \\ \mathbf{0} \end{bmatrix} + \begin{bmatrix} \mathbf{0} \\ \mathbf{CABu} \end{bmatrix} + \begin{bmatrix} \mathbf{0} \\ \mathbf{CA}(\mathbf{A}\mathbf{x} + \mathbf{N}\mathbf{f}) + \mathbf{C}\mathbf{N}\dot{\mathbf{f}} \end{bmatrix} \\ &= \begin{bmatrix} \mathbf{0} & \mathbf{I} \\ \mathbf{0} & \mathbf{0} \end{bmatrix}\mathbf{z} + \begin{bmatrix} \mathbf{0} \\ \mathbf{CAB} \end{bmatrix}\mathbf{u} + \begin{bmatrix} \mathbf{0} \\ \mathbf{I} \end{bmatrix}\mathbf{f}_g, \end{aligned} \tag{15}$$

where $\mathbf{f}_g$ is defined as the generalized-disturbance vector and expressed as

$$\mathbf{f}_g = \mathbf{C}\left[\mathbf{A}(\mathbf{A}\mathbf{x} + \mathbf{N}\mathbf{f}) + \mathbf{N}\dot{\mathbf{f}}\right]. \tag{16}$$

Therefore, the generalized-disturbance vector $\mathbf{f}_g$ is obtained in the refined state space model, of which $\mathbf{z}$ is the state vector. It is obvious that all physical disturbances and their influence matrices are included in the generalized-disturbance vector. Then the physical disturbances can be indirectly counteracted by feeding back estimated generalized disturbances through the GDR controller, if the generalized disturbances can be

estimated. According to (15), the refined state space model is derived as

$$\dot{\mathbf{z}} = \widetilde{\mathbf{A}}\mathbf{z} + \widetilde{\mathbf{B}}\mathbf{u} + \widetilde{\mathbf{N}}\mathbf{f}_g, \tag{17}$$

$$\mathbf{y} = \widetilde{\mathbf{C}}\mathbf{z}, \tag{18}$$

where $\mathbf{u}$ and $\mathbf{y}$ are the control vector and output vector which are exactly identical to those of the original state space model in (3) and (4). Furthermore, $\widetilde{\mathbf{A}}$, $\widetilde{\mathbf{B}}$, $\widetilde{\mathbf{N}}$, and $\widetilde{\mathbf{C}}$ denote the system matrix, control input matrix, generalized-disturbance influence matrix, and output matrix of the refined state space model, respectively, which are expressed as

$$\widetilde{\mathbf{A}} = \begin{bmatrix} \mathbf{0} & \mathbf{I} \\ \mathbf{0} & \mathbf{0} \end{bmatrix}, \tag{19}$$

$$\widetilde{\mathbf{B}} = \begin{bmatrix} \mathbf{0} \\ \mathbf{CAB} \end{bmatrix}, \tag{20}$$

$$\widetilde{\mathbf{N}} = \begin{bmatrix} \mathbf{0} \\ \mathbf{I} \end{bmatrix}, \tag{21}$$

$$\widetilde{\mathbf{C}} = \begin{bmatrix} \mathbf{I} & \mathbf{0} \end{bmatrix}. \tag{22}$$

Transformed from the original state space model, the refined state space model describes the smart structure system in a simpler structure by using state vector $\mathbf{z}$. From the derivation of the refined state space model, it can be seen that there is no information lost during the transformation, which means that the dynamic relations between inputs, physical disturbances, and outputs of the smart structure system described by the refined state space model are exactly the same as those described by the original state space model.

Compared to the original state space model, the refined state space model is different mainly in three parts. The first is integrating all the physical disturbances and their influence matrices into generalized disturbances, which brings advantages in observer and controller design and therefore in estimation and counteraction of physical disturbances. It is apparent that the generalized-disturbance influence matrix $\widetilde{\mathbf{N}}$ is known; thus a PI or GPI observer can be built to estimate the generalized disturbances. This means that the physical disturbances can be counteracted indirectly by feeding back estimated generalized disturbances, no matter whether the influence matrices of physical disturbances are known or not, which is impossible in the original state space model. Secondly, the structure of the refined state space model is much simpler than the original one since the coupled state variables are also integrated into the generalized disturbances. As a result, the refined system can be decoupled easily so that it is much easier to design high performance observer and controller, which leads to more accurate estimation and counteraction of periodic disturbances with unknown high-order frequencies or random disturbances varying fast. The third is the utilization of the new state vector $\mathbf{z}$, which removes the limitation of conventional DR control that the number of sensor signals can not be less than the number of disturbances. From (16), it can be found out that the number of generalized disturbances is equal to the number of system outputs, namely, the number of sensor signals. Therefore the generalized disturbances can be observed in the refined state space model, whether or not the number of sensor signals is less than that of physical disturbances. Moreover, it can be seen from (5) that the model dimension of the original state space model is twice the dimension of the smart structure's FE model, which can be very large when the model is complex. In contrast, the model dimension of the refined state space model is only twice the number of system outputs, as seen in (13). Apparently the model dimension of the refined state space model is much smaller in most cases, which means the computational cost is reduced by using the refined state space model.

3.2. Observer Design

3.2.1. Extended System. Normally observers are designed for observing system state variables but not disturbances. However, in the PI and GPI observer, disturbance estimation is achieved by observing virtual state variables which are used to approximate disturbances. Therefore, to estimate the generalized disturbances, firstly, the relation between generalized disturbances and state variables is assumed as [64, 65]

$$\mathbf{f}_g(t) = \mathbf{H}\mathbf{v}(t) + \boldsymbol{\Delta}(t), \tag{23}$$

$$\dot{\mathbf{v}}(t) = \mathbf{V}\mathbf{v}(t). \tag{24}$$

Here, the generalized-disturbance vector $\mathbf{f}_g(t)$ is divided into a linear part $\mathbf{Hv}(t)$ and a residual error part $\boldsymbol{\Delta}(t)$. The former $\mathbf{Hv}(t)$ functions as the approximation of the generalized disturbances while the latter $\boldsymbol{\Delta}(t)$ is assumed to be small and negligible in most cases. In the linear part, $\mathbf{H}$ is a coefficient matrix and $\mathbf{v}(t)$ is the virtual state vector comprised of finite base functions. Subsequently, an extended system integrating state vectors $\mathbf{z}$ and $\mathbf{v}$ is built. Substituting (23) and (24) into (17) and (18), the extended system is obtained as

$$\begin{Bmatrix} \dot{\mathbf{z}} \\ \dot{\mathbf{v}} \end{Bmatrix} = \begin{bmatrix} \widetilde{\mathbf{A}} & \widetilde{\mathbf{N}}\mathbf{H} \\ \mathbf{0} & \mathbf{V} \end{bmatrix} \begin{Bmatrix} \mathbf{z} \\ \mathbf{v} \end{Bmatrix} + \begin{bmatrix} \widetilde{\mathbf{B}} \\ \mathbf{0} \end{bmatrix} \mathbf{u} + \begin{bmatrix} \widetilde{\mathbf{N}} \\ \mathbf{0} \end{bmatrix} \boldsymbol{\Delta}, \tag{25}$$

$$\mathbf{y} = \begin{bmatrix} \widetilde{\mathbf{C}} & \mathbf{0} \end{bmatrix} \begin{Bmatrix} \mathbf{z} \\ \mathbf{v} \end{Bmatrix}. \tag{26}$$

Obviously, generalized disturbances are approximated by virtual state variables in the extended system. As a result, generalized disturbances can be estimated through a state observer of the extended system, which is built in the next section.

It is manifest from (23) and (24) that $\mathbf{H}$ and $\mathbf{V}$ determine the dynamic behavior of estimated generalized disturbances, which is fundamental to the disturbance tracking performance of the observer. To choose an appropriate set of $\mathbf{H}$ and $\mathbf{V}$, a fictitious disturbance model that has similar dynamic behavior to the disturbance signal is helpful to obtain better tracking performance of the observer. For example, cosine functions with same frequencies as those of disturbances are utilized in the fictitious disturbance model of GPI observer,

which leads to improvement in tracking performance of periodic disturbances with known frequencies. Nonetheless, the physical disturbances are assumed to be totally unknown in this paper, which means it is impossible to get any dynamic information of the physical and generalized disturbances. Hence, a plain fictitious disturbance model with no extra dynamic information but just step functions is adopted, which leads to a PI observer [64, 70]. In the PI observer, the fictitious model of generalized disturbance and the virtual state vector are assumed as

$$\mathbf{f}_g \approx \begin{bmatrix} a_{10} \\ a_{20} \\ \cdots \\ a_{m0} \end{bmatrix}, \qquad \mathbf{v} = \begin{bmatrix} a_{10} \\ a_{20} \\ \cdots \\ a_{m0} \end{bmatrix} \tag{27}$$

which leads to

$$\mathbf{H} = \mathbf{I}, \qquad \mathbf{V} = \mathbf{0}. \tag{28}$$

3.2.2. Observer Gain Design. According to the standard Luenberger observer, a state observer for the extended system in (25) and (26), namely, the PI observer, is constructed as

$$\begin{Bmatrix} \dot{\widehat{\mathbf{z}}} \\ \dot{\widehat{\mathbf{v}}} \end{Bmatrix} = \begin{bmatrix} \widetilde{\mathbf{A}} & \widetilde{\mathbf{N}}\mathbf{H} \\ \mathbf{0} & \mathbf{V} \end{bmatrix} \begin{Bmatrix} \widehat{\mathbf{z}} \\ \widehat{\mathbf{v}} \end{Bmatrix} + \begin{bmatrix} \widetilde{\mathbf{B}} \\ \mathbf{0} \end{bmatrix} \mathbf{u} + \begin{bmatrix} \mathbf{L}_z \\ \mathbf{L}_v \end{bmatrix} (\mathbf{y} - \widehat{\mathbf{y}}), \tag{29}$$

$$\widehat{\mathbf{y}} = \begin{bmatrix} \widetilde{\mathbf{C}} & \mathbf{0} \end{bmatrix} \begin{Bmatrix} \widehat{\mathbf{z}} \\ \widehat{\mathbf{v}} \end{Bmatrix}, \tag{30}$$

where $\mathbf{L}_z$ and $\mathbf{L}_v$ denote observer gains. In order to stabilize the observer system, the estimation error of the PI observer must converge to zero. Define the estimation error of the state vectors in (25) as

$$\mathbf{e}_z = \mathbf{z} - \widehat{\mathbf{z}}, \qquad \mathbf{e}_v = \mathbf{v} - \widehat{\mathbf{v}}. \tag{31}$$

Succeedingly the estimation error model of the GD observer in (29) can be acquired as

$$\begin{Bmatrix} \dot{\mathbf{e}}_z \\ \dot{\mathbf{e}}_v \end{Bmatrix} = \mathbf{A}_b \begin{Bmatrix} \mathbf{e}_z \\ \mathbf{e}_v \end{Bmatrix} + \begin{bmatrix} \widetilde{\mathbf{N}} \\ \mathbf{0} \end{bmatrix} \boldsymbol{\Delta}, \tag{32}$$

where $\mathbf{A}_b$ is the system matrix of the estimation error model and can be expressed as

$$\mathbf{A}_b = \begin{bmatrix} \widetilde{\mathbf{A}} - \mathbf{L}_z\widetilde{\mathbf{C}} & \widetilde{\mathbf{N}}\mathbf{H} \\ -\mathbf{L}_v\widetilde{\mathbf{C}} & \mathbf{V} \end{bmatrix}. \tag{33}$$

It is evident that the estimation error system given in (32) will be stable if $\boldsymbol{\Delta}$ is bounded and all eigenvalues of $\mathbf{A}_b$ are placed in the left half plane. As a result, the estimation errors $\mathbf{e}_z$ and $\mathbf{e}_v$ will converge to zero, which means the state variables observed by the PI observer in (29) and (30) will converge to the real ones given in (25) and (26). Substituting (19), (21), (22), and (28) into (33), $\mathbf{A}_b$ is formed as

$$\mathbf{A}_b = \begin{bmatrix} -\mathbf{L}_{z1} & \mathbf{I} & \mathbf{0} \\ -\mathbf{L}_{z2} & \mathbf{0} & \mathbf{I} \\ -\mathbf{L}_v & \mathbf{0} & \mathbf{0} \end{bmatrix} \tag{34}$$

with

$$\mathbf{L}_z = \begin{bmatrix} \mathbf{L}_{z1} \\ \mathbf{L}_{z2} \end{bmatrix}. \tag{35}$$

Accordingly, the characteristic polynomial of $\mathbf{A}_b$ can be expressed as

$$\left|s\mathbf{I} - \mathbf{A}_b\right| = \begin{vmatrix} s\mathbf{I} + \mathbf{L}_{z1} & -\mathbf{I} & \mathbf{0} \\ \mathbf{L}_{z2} & s\mathbf{I} & -\mathbf{I} \\ \mathbf{L}_v & 0 & s\mathbf{I} \end{vmatrix}. \tag{36}$$

Applying elementary row operations, the determinant above is calculated as

$$\begin{aligned} \left|s\mathbf{I} - \mathbf{A}_b\right| &= \begin{vmatrix} s\mathbf{I} + \mathbf{L}_{z1} + \dfrac{\mathbf{L}_{z2}}{s} + \dfrac{\mathbf{L}_v}{s^2} & \mathbf{0} & \mathbf{0} \\ \mathbf{L}_{z2} + \dfrac{\mathbf{L}_v}{s} & s\mathbf{I} & \mathbf{0} \\ \mathbf{L}_v & \mathbf{0} & s\mathbf{I} \end{vmatrix} \\ &= \left|s^3\mathbf{I} + s^2\mathbf{L}_{z1} + s\mathbf{L}_{z2} + \mathbf{L}_v\right|. \end{aligned} \tag{37}$$

For the convenience of pole placement, the observer system needs to be decoupled by assuming gain matrices $\mathbf{L}_{z1}$, $\mathbf{L}_{z2}$, and $\mathbf{L}_v$ to be diagonal matrices expressed as

$$\begin{aligned} \mathbf{L}_{z1} &= \operatorname{diag}(l_{11}, l_{12}, \ldots, l_{1m}), \\ \mathbf{L}_{z2} &= \operatorname{diag}(l_{21}, l_{22}, \ldots, l_{2m}), \\ \mathbf{L}_v &= \operatorname{diag}(l_{31}, l_{32}, \ldots, l_{3m}), \end{aligned} \tag{38}$$

which leads to

$$\left|s\mathbf{I} - \mathbf{A}_b\right| = \prod_{i=1}^{m} \left(s^3 + l_{1i}s^2 + l_{2i}s + l_{3i}\right). \tag{39}$$

The roots of (39) can be arranged according to the classical third-order system as

$$\left|s\mathbf{I} - \mathbf{A}_b\right| = \prod_{i=1}^{m} \left(s + \frac{1}{T_{oi}}\right)^3, \tag{40}$$

where T_{oi} is an observer gain parameter which is proportional to the settling time of the ith third-order system [71]. Hence the settling time of the estimation error system composed

of m parallel third-order systems is positively related to the maximum of T_{oi} $(i = 1, 2, \ldots, m)$. Apparently, $-1/T_{oi}$ denotes the ith eigenvalue of $\mathbf{A}_b$, that is, the value of ith pole of the estimation error system given in (32). All the poles will be placed in the left half plane if

$$T_{oi} > 0, \quad (i = 1, 2, \ldots, m). \tag{41}$$

Consequently, the observer gain matrices are obtained as

$$\begin{aligned}
\mathbf{L}_{z1} &= \operatorname{diag}\left(\frac{3}{T_{o1}}, \frac{3}{T_{o2}}, \ldots, \frac{3}{T_{om}}\right),\\
\mathbf{L}_{z2} &= \operatorname{diag}\left(\frac{3}{T_{o1}^2}, \frac{3}{T_{o2}^2}, \ldots, \frac{3}{T_{om}^2}\right),\\
\mathbf{L}_{v} &= \operatorname{diag}\left(\frac{1}{T_{o1}^3}, \frac{1}{T_{o2}^3}, \ldots, \frac{1}{T_{om}^3}\right).
\end{aligned} \tag{42}$$

The definition of settling time is the time required for the response signal to settle to within a certain percent (2% or 5%) of its final value [71]. That is to say, the settling time determines the response speed or the converging speed of the estimation error system. Theoretically, the shorter the settling time is, the faster the PI observer converges, and the quicker the generalized disturbances can be estimated. Additionally, the minimum of settling time is commonly limited by restrictions like sensor noise and sampling rate in practice.

Compared to the conventional DR control [64, 70], the observer design and tuning processes in GDR control are simpler and more intuitive. Since the coupled state variables are integrated in the generalized-disturbance vector, the refined state space model is much easier to decouple, which facilitates the closed-loop design of the observer. Using pole placement method, the PI observer is designed as a critically damped structure with gain parameters significantly correlated with the response speed of the PI observer, which is proven in the following simulation of the PI observer. Hence the PI observer can be tuned more intuitively to obtain the desired disturbance tracking performance in GDR control.

3.3. Controller Design. With the PI observer properly designed, the estimated generalized disturbances are fed to the DR controller with state vector $\mathbf{z}$ to suppress vibrations. Unlike DR-PI or DR-GPI control, the state vector $\mathbf{z}$ in the GDR control is composed of $\mathbf{y}$ and $\dot{\mathbf{y}}$, which can be obtained directly from the output vector of the original plant without estimation. As a consequence, the GDR control owns an advantage over the conventional DR control, which is feeding more accurate state variables back to the system. The control law is designed as

$$\mathbf{u} = -\mathbf{K}_z\mathbf{z} - \mathbf{K}_v\hat{\mathbf{v}}, \tag{43}$$

where $\mathbf{K}_z$ and $\mathbf{K}_v$ denote the gain matrices for vectors $\mathbf{z}$ and $\hat{\mathbf{v}}$, respectively. In order to design the controller gains in a clear way, the gain matrices are decomposed as

$$\begin{aligned}
\mathbf{K}_z &= \mathbf{B}_{cr}^{-}\widetilde{\mathbf{K}}_z,\\
\mathbf{K}_v &= \mathbf{B}_{cr}^{-}\widetilde{\mathbf{K}}_v
\end{aligned} \tag{44}$$

with

$$\begin{aligned}
\mathbf{B}_c\mathbf{B}_{cr}^{-} &= \mathbf{I},\\
\mathbf{B}_c &= \mathbf{CAB}.
\end{aligned} \tag{45}$$

Here, $\mathbf{B}_c$ is the nonzero part of $\widetilde{\mathbf{B}}$, and $\mathbf{B}_{cr}^{-}$ is the right inverse of $\mathbf{B}_c$, which leads to

$$\widetilde{\mathbf{B}}\mathbf{B}_{cr}^{-} = \begin{bmatrix}\mathbf{0}\\ \mathbf{B}_c\end{bmatrix}\mathbf{B}_{cr}^{-} = \begin{bmatrix}\mathbf{0}\\ \mathbf{I}\end{bmatrix} = \widetilde{\mathbf{N}}. \tag{46}$$

The necessary and sufficient condition for the existence of $\mathbf{B}_{cr}^{-}$ is that $\mathbf{B}_c$ is a row full-rank matrix, which is normally satisfied in smart structure systems. Substituting (43)–(45) into (17), the state equation of the closed-loop system of the refined model is obtained as

$$\begin{aligned}
\dot{\mathbf{z}} &= \widetilde{\mathbf{A}}\mathbf{z} - \widetilde{\mathbf{B}}\mathbf{B}_{cr}^{-}\widetilde{\mathbf{K}}_z\mathbf{z} - \widetilde{\mathbf{B}}\mathbf{B}_{cr}^{-}\widetilde{\mathbf{K}}_v\hat{\mathbf{v}} + \widetilde{\mathbf{N}}\mathbf{f}_g\\
&= \widetilde{\mathbf{A}}_c\mathbf{z} + \widetilde{\mathbf{N}}\left(\mathbf{f}_g - \widetilde{\mathbf{K}}_v\hat{\mathbf{v}}\right)
\end{aligned} \tag{47}$$

with

$$\widetilde{\mathbf{A}}_c = \widetilde{\mathbf{A}} - \widetilde{\mathbf{N}}\widetilde{\mathbf{K}}_z, \tag{48}$$

where $\widetilde{\mathbf{A}}_c$ is the system matrix of the closed-loop state space model. According to (23), $\mathbf{f}_g$ can be counteracted by $\widetilde{\mathbf{K}}_v\hat{\mathbf{v}}$ if

$$\widetilde{\mathbf{K}}_v = \mathbf{H}, \tag{49}$$

which leads to

$$\dot{\mathbf{z}} = \widetilde{\mathbf{A}}_c\mathbf{z} + \widetilde{\mathbf{N}}\left(\mathbf{He}_v + \boldsymbol{\Delta}\right). \tag{50}$$

Owing to the convergent PI observer, the estimation error $\mathbf{e}_v$ is bounded, as well as for the residual error $\boldsymbol{\Delta}$. Hence the closed-loop system will be asymptotically stable if all its poles are placed on the left half plane. Assuming $\widetilde{\mathbf{K}}_z$ as

$$\widetilde{\mathbf{K}}_z = \begin{bmatrix}\widetilde{\mathbf{K}}_{z1} & \widetilde{\mathbf{K}}_{z2}\end{bmatrix}, \tag{51}$$

then substituting (19), (21), and (51) into (48), $\widetilde{\mathbf{A}}_c$ can be acquired as

$$\widetilde{\mathbf{A}}_c = \begin{bmatrix}\mathbf{0} & \mathbf{I}\\ -\widetilde{\mathbf{K}}_{z1} & -\widetilde{\mathbf{K}}_{z2}\end{bmatrix}. \tag{52}$$

The control gains can be designed in a decoupling way similar to the observer design. Firstly, applying elementary column operations, the characteristic polynomial of $\widetilde{\mathbf{A}}_c$ is derived as

$$\left|s\mathbf{I} - \widetilde{\mathbf{A}}_c\right| = \left|s^2\mathbf{I} + s\widetilde{\mathbf{K}}_{z2} + \widetilde{\mathbf{K}}_{z1}\right|. \tag{53}$$

Secondly, the matrices $\widetilde{\mathbf{K}}_{z1}$ and $\widetilde{\mathbf{K}}_{z2}$ are assumed to be diagonal as

$$\begin{aligned}
\widetilde{\mathbf{K}}_{z1} &= \operatorname{diag}\left(k_{11}, k_{12}, \ldots, k_{1m}\right),\\
\widetilde{\mathbf{K}}_{z2} &= \operatorname{diag}\left(k_{21}, k_{22}, \ldots, k_{2m}\right).
\end{aligned} \tag{54}$$

Finally, the determinant above can be expressed as

$$\left|s\mathbf{I} - \widetilde{\mathbf{A}}_c\right| = \prod_{i=1}^{m}\left(s^2 + k_{2i}s + k_{1i}\right). \tag{55}$$

According to the classical second-order system, controller gains can be designed as

$$\begin{aligned} k_{2i} &= \frac{2\zeta}{T_{ci}}, \\ k_{1i} &= \frac{1}{T_{ci}^2}, \\ &(i = 1, 2, \ldots, m), \end{aligned} \tag{56}$$

where T_{ci} is a controller gain parameter which is proportional to the settling time of the ith second-order system in (55) and ζ denotes the damping ratio [71]. Therefore, m pairs of poles can be placed in the left half plane as

$$s = -\frac{1}{T_{ci}}\left(\zeta \pm j\sqrt{1-\zeta^2}\right), \quad (i = 1, 2, \ldots, m) \tag{57}$$

with

$$\begin{aligned} \zeta &> 0, \\ T_{ci} &> 0 \end{aligned} \tag{58}$$

in which j represents the unit imaginary number. Furthermore, ζ is usually set as 1 to make the closed-loop system critically damped. Alternatively, 0.707 is also a good choice for its shortest settling time and acceptable overshoot within 5% [71]. Analogous to the observer design, the settling time of the closed-loop system is positively related to the maximum of T_{ci} $(i = 1, 2, \ldots, m)$ and determines the response speed of the closed-loop system. For that reason, the values of T_{ci} need to be small enough to get a desired control result. Moreover, it is easy to find out that the GDR controller developed above will turn into a proportional-derivative (PD) controller if $\mathbf{K}_v = 0$, which is compared with GDR control in later simulations.

3.4. Closed-Loop System. Substituting (43) into (3), (25), and (29), the closed-loop GDR control system with PI observer is obtained as

$$\begin{Bmatrix} \dot{\mathbf{x}} \\ \dot{\mathbf{z}} \\ \dot{\hat{\mathbf{z}}} \\ \dot{\hat{\mathbf{v}}} \end{Bmatrix} = \begin{bmatrix} \mathbf{A} & -\mathbf{B}\mathbf{B}_{cr}^{-}\widetilde{\mathbf{K}}_z & \mathbf{0} & -\mathbf{B}\mathbf{B}_{cr}^{-}\widetilde{\mathbf{K}}_v \\ \widetilde{\mathbf{N}}\mathbf{C}\mathbf{A}^2 & \widetilde{\mathbf{A}} - \widetilde{\mathbf{N}}\widetilde{\mathbf{K}}_z & \mathbf{0} & -\widetilde{\mathbf{N}}\widetilde{\mathbf{K}}_v \\ \mathbf{0} & \mathbf{L}_z\widetilde{\mathbf{C}} - \widetilde{\mathbf{N}}\widetilde{\mathbf{K}}_z & \widetilde{\mathbf{A}} - \mathbf{L}_z\widetilde{\mathbf{C}} & \widetilde{\mathbf{N}}\mathbf{H} - \widetilde{\mathbf{N}}\widetilde{\mathbf{K}}_v \\ \mathbf{0} & \mathbf{L}_v\widetilde{\mathbf{C}} & -\mathbf{L}_v\widetilde{\mathbf{C}} & \mathbf{V} \end{bmatrix} \begin{Bmatrix} \mathbf{x} \\ \mathbf{z} \\ \hat{\mathbf{z}} \\ \hat{\mathbf{v}} \end{Bmatrix} + \begin{bmatrix} \mathbf{N} \\ \widetilde{\mathbf{N}}\mathbf{C}\mathbf{A}\mathbf{N} \\ \mathbf{0} \\ \mathbf{0} \end{bmatrix} \mathbf{f}, \quad \mathbf{y} = \begin{bmatrix} \mathbf{C} & \mathbf{0} & \mathbf{0} & \mathbf{0} \end{bmatrix} \begin{Bmatrix} \mathbf{x} \\ \mathbf{z} \\ \hat{\mathbf{z}} \\ \hat{\mathbf{v}} \end{Bmatrix} \tag{59}$$

with the control input expressed as

$$\mathbf{u} = \begin{bmatrix} \mathbf{0} & -\mathbf{B}_{cr}^{-}\widetilde{\mathbf{K}}_z & \mathbf{0} & -\mathbf{B}_{cr}^{-}\widetilde{\mathbf{K}}_v \end{bmatrix} \begin{Bmatrix} \mathbf{x} \\ \mathbf{z} \\ \hat{\mathbf{z}} \\ \hat{\mathbf{v}} \end{Bmatrix}. \tag{60}$$

For the purpose of observer performance analysis, a closed-loop observer system in which $\mathbf{f}_g$ and $\widehat{\mathbf{f}}_g$ are, respectively, taken as input and output vectors is needed. Substituting (43) into (25) and (29), the closed-loop observer system is expressed as

$$\begin{Bmatrix} \dot{\mathbf{z}} \\ \dot{\hat{\mathbf{z}}} \\ \dot{\hat{\mathbf{v}}} \end{Bmatrix} = \begin{bmatrix} \widetilde{\mathbf{A}} - \widetilde{\mathbf{N}}\widetilde{\mathbf{K}}_z & \mathbf{0} & -\widetilde{\mathbf{N}}\widetilde{\mathbf{K}}_v \\ \mathbf{L}_z\widetilde{\mathbf{C}} - \widetilde{\mathbf{N}}\widetilde{\mathbf{K}}_z & \widetilde{\mathbf{A}} - \mathbf{L}_z\widetilde{\mathbf{C}} & \widetilde{\mathbf{N}}\mathbf{H} - \widetilde{\mathbf{N}}\widetilde{\mathbf{K}}_v \\ \mathbf{L}_v\widetilde{\mathbf{C}} & -\mathbf{L}_v\widetilde{\mathbf{C}} & \mathbf{V} \end{bmatrix} \begin{Bmatrix} \mathbf{z} \\ \hat{\mathbf{z}} \\ \hat{\mathbf{v}} \end{Bmatrix} + \begin{bmatrix} \widetilde{\mathbf{N}} \\ \mathbf{0} \\ \mathbf{0} \end{bmatrix} \mathbf{f}_g, \quad \widehat{\mathbf{f}}_g = \{\mathbf{0} \quad \mathbf{0} \quad \mathbf{H}\} \begin{Bmatrix} \mathbf{z} \\ \hat{\mathbf{z}} \\ \hat{\mathbf{v}} \end{Bmatrix}. \tag{61}$$

4. Simulation Results

The GDR control with PI observer is implemented numerically on a cantilevered smart beam which is bonded with two collocated piezoceramic patches on both surfaces, as shown in Figure 1. The two patches are polarized in opposite directions along the θ^3 axis so that one piezoelectric patch functions as an actuator while the other one as a sensor. Disturbance forces are applied in the direction of axis θ^3 at one or two points among points P_1, P_2, and P_3, which are equidistantly located on axis θ^1 starting from the tip node of the smart beam. The geometrical dimensions and material properties of the steel beam and piezoceramic patches are listed in Tables 1 and 2.

Considering the linear variant of FOSD plate theory [64], a piezoelectric coupled FE model for the smart beam in Figure 1 is built with a 5×1 mesh and an eight-node

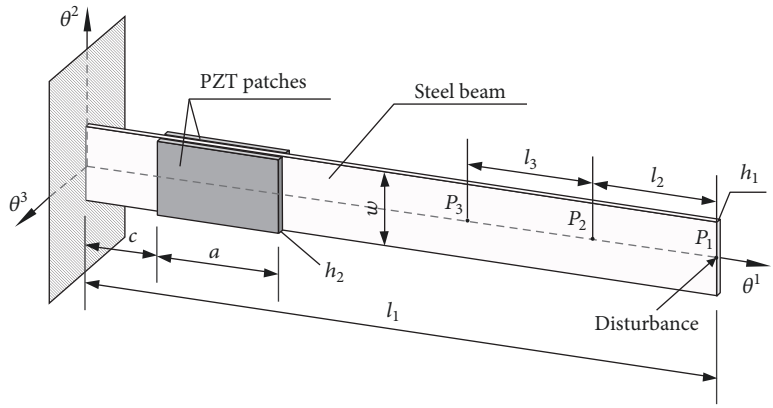

Figure 1: Cantilevered beam bonded with piezoelectric patches.

Table 1: Geometrical dimensions of the steel beam and PZT patches.

Property	Steel beam	PZT patches
Length (mm)	$l_1 = 350$	$a = 75$
Width (mm)	$w = 25$	$w = 25$
Height (mm)	$h_1 = 0.8$	$h_2 = 0.25$
Location (mm)	–	$c = 50$
Spacing of P_1, P_2, P_3 (mm)	$l_2 = l_3 = 70$	–

Serendipity shell element. The first five eigenfrequencies are displayed in Table 3, and the first two eigenfrequencies are used as the frequencies of disturbance forces in later simulations.

4.1. Observer Performance Analysis. In this section, the disturbance tracking capabilities of the PI observer in GDR control, as well as those of the PI and GPI observers in DR control, are compared and analyzed through a step disturbance estimation and a Bode diagram. For simplicity, the names of these three observers are abbreviated to PI (GDR), PI (DR), and GPI (DR), respectively. In the aspect of GDR control, the closed-loop system of the PI (GDR) observer given in (61) is adopted in these two simulations. The gain parameter of the PI (GDR) observer T_o is set with five different values from 0.2×10^{-3} to 3.2×10^{-3}. On the other hand, according to the analysis of PI (DR) and GPI (DR) observers in the work of Zhang et al. [64], the gain parameter of these two observers, namely, b, is recommended as $b = 100$ for a short rise time and small overshoot.

For a start, a step signal with amplitude of 0.1 is given as the disturbance or generalized disturbance for estimation. Thereafter, the estimated disturbance signals are compared in response speed. As shown in Figure 2, overshoots are found in the signals estimated by PI (DR) and GPI (DR) observers, while not in any signals estimated by the PI (GDR) observers due to the critically damped structure of PI (GDR) observer. As described in pole placement procedure, the response speed of PI (GDR) observer obviously gets faster with the decrease of T_o, which proved the point that the gain parameters of PI (GDR) observer is significantly correlated with the response speed. Apparently, the PI (GDR) observer can be tuned trivially by decreasing T_o, and the GD observer responses much faster than the PI (DR) and GPI (DR) ones when $T_o < 0.8 \times 10^{-3}$. On the other hand, although the gain parameter of PI (DR) and GPI (DR) observers b is positively correlated with the observer response speed, the improvement in the response speeds of PI (DR) and GPI (DR) observers is not that obvious when b increases, and the Riccati equation may become unsolvable if b is excessively large, which is referred to in [64]. In the later simulations, gain parameter $b = 100$ is applied to the PI (DR) and GPI (DR) observers if it is not mentioned otherwise.

In the Bode diagram shown in Figure 3, the three observers with the same parameters as those in the step estimation simulation are analyzed in frequency domain. Obviously, the frequency response magnitudes of PI (DR) and GPI (DR) observers begin to decay seriously after 20 rad/s, which means undervalued estimation. On the other side, the frequency response magnitude of the PI (GDR) observer with parameter $T_o = 0.2 \times 10^{-3}$ does not show obvious decay until 1×10^3 rad/s. Additionally, the PI (GDR) observer is proved to be a minimum phase system according to the phase plot in Figure 3 while the PI (DR) and GPI (DR) observers are nonminimum phase systems, which are more difficult to stabilize than the minimum one. The PI (GDR) observer also keeps its phase lag small in a frequency range much wider than those of PI (DR) and GPI (DR) observers, which means the PI (GDR) observer is able to estimate higher frequency disturbances with small time delay. To summarize, the response speed of PI (GDR) observer is significantly correlated with the gain parameter T_o, and, according to the frequency response magnitudes and phase lags of the three observers, the PI (GDR) observer starts to show better disturbance tracking capability than the other two observers when $T_o < 0.8 \times 10^{-3}$.

4.2. Closed-Loop System Performance Analysis. In order to analyze the influence of observer and controller gain parameters on the closed-loop system performance, frequency responses of uncontrolled and controlled closed-loop systems with different gain parameters are calculated. Since the GDR

Table 2: Material properties of the steel beam and PZT patches.

Property	Symbol	Steel beam	PZT patches
Young's Modulus (GPa)	Y	210	67
Density (kg/m^3)	ρ	7900	7800
Poisson's ratio	ν	0.3	0.3
Piezoelectric coefficient (C/N)	d_{31}, d_{32}	–	-2.1×10^{-10}
Permittivity (F/m)	ϵ_{33}	–	2.13×10^{-8}

Table 3: First five eigenfrequencies of the cantilevered smart beam (Hz).

Mesh	Mode 1	Mode 2	Mode 3	Mode 4	Mode 5
5×1	6.2144	35.0444	110.1355	176.5464	178.0647

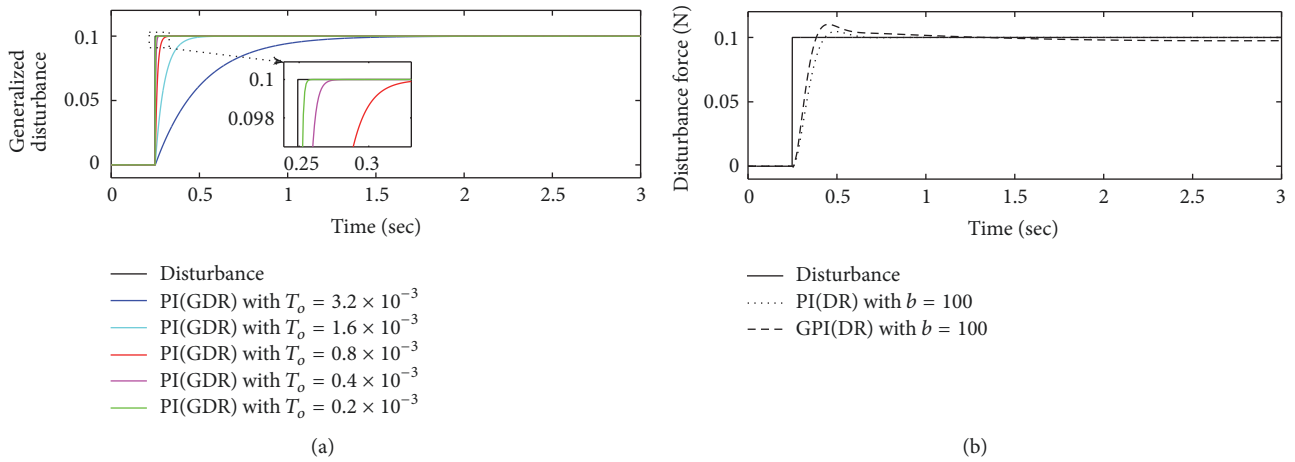

Figure 2: Estimated step disturbances by PI (DR), GPI (DR), and PI (GDR) observers with different gain parameters.

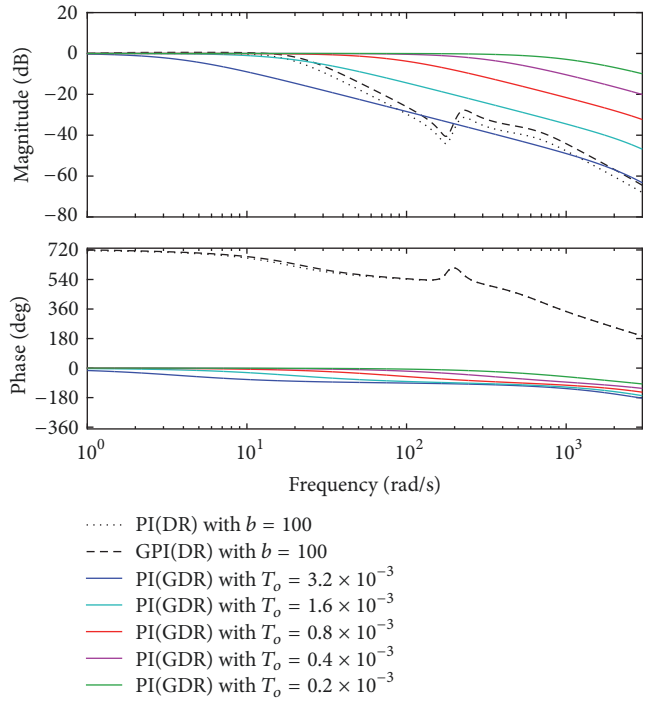

Figure 3: The Bode diagram for PI (DR), GPI (DR), and PI (GDR) observers with different gain parameters.

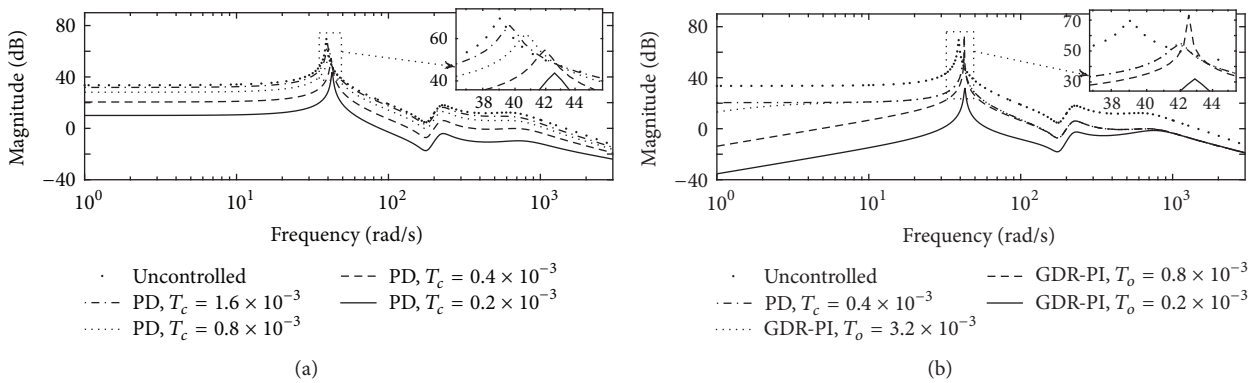

FIGURE 4: The frequency responses of the controlled and uncontrolled smart beam: (a) PD control configured with different T_c and (b) PD control and GDR control with PI observers configured with $T_c = 0.4 \times 10^{-3}$ and different T_o.

control with PI observer will be simplified to a PD control when there are no estimated disturbances fed back, PD controllers with different controller gain parameters T_c are firstly analyzed by employing the closed-loop system in (59) with $\mathbf{K}_v = 0$. Afterwards GDR controllers with PI observer configured by $T_c = 0.4 \times 10^{-3}$ and different T_o are compared with a PD controller using the same T_c. On one hand, the influence of controller gain on the closed-loop system performance can be analyzed through the comparison of PD controllers with different gain parameters. On the other hand, the frequency characteristics of closed-loop systems of PD and GDR control as well as the relation between the closed-loop system performance and the observer gain parameters can be analyzed through the comparison between frequency responses of PD control and GDR control.

As shown in Figure 4(a), the response magnitudes of all closed-loop systems of PD control are reduced for low and high frequency disturbances, which means the influence of disturbance is attenuated by the PD controller, evenly throughout the frequency range from 1 rad/s to 2×10^3 rad/s. Furthermore, the response magnitude of closed-loop system of PD control keeps reducing with the decrease of T_c. Similarly, in Figure 4(b), smaller response magnitude of the closed-loop system of GDR-PI control, that is, better closed-loop system performance of GDR-PI control, is achieved by a smaller T_o, which means feeding back accurately estimated generalized disturbances improves the closed-loop system performance. Compared to the PD control, the response magnitudes of GDR-PI control are much smaller in low frequency range. However, when it comes to high frequency, the GDR-PI control performs equally or even worse at some point. This is caused by feeding back incorrect estimations of high frequency disturbances. According to (42), the value of T_o is negatively correlated with the observer gains and converging speed of the PI (GDR) observer. Therefore, the smaller T_o is, the higher the frequency of disturbance can be accurately estimated and counteracted, and the wider the frequency range in which the GDR-PI control can get better performance than the PD control with the same T_c. As shown in Figure 4(b), the GDR-PI control with $T_o = 0.2 \times 10^{-3}$ performs much better than the PD one in a frequency range up to 500 rad/s, which is far more enough to cover the first two eigenfrequencies of the smart beam. Therefore, $T_c = 0.4 \times 10^{-3}$ and $T_o = 0.2 \times 10^{-3}$ are adopted in later simulations to, respectively, supply proper damping for disturbances with frequency over 500 rad/s and excellent disturbance rejection for those within 500 rad/s. In conclusion, feeding back accurately estimated generalized disturbances evidently improves the disturbance rejection performance of GDR-PI control in a limited frequency range, and, with the increase of observer gains, higher ceiling of the frequency range and greater improvement of disturbance rejection performance can be obtained.

4.3. Vibration Suppression with Different Disturbances. To testify the vibration suppression performance of GDR-PI control in the specified situations mentioned at the beginning of this paper, the following vibration suppression simulations are implemented, respectively, considering four situations as follows: (i) the disturbance force influence matrix $\mathbf{N}$ is unknown; (ii) the number of disturbance forces is greater than the number of senor signals; (iii) the disturbance force is periodic but its frequency is unknown; (iv) the disturbance force is random and varies fast. For comparison, DR-GPI control and H_∞ state feedback control are also applied in the following simulations.

4.3.1. Disturbance with Unknown Influence Matrix. Firstly, the three control strategies are validated by two simulations in which the cantilevered smart beam is excited by a harmonic disturbance force with unknown influence matrix. In these two simulations, the acting point of disturbance force, which determines the disturbance influence matrix, is assumed to be unknown but actually at point P_2. However, the DR-GPI control cannot be implemented without the disturbance influence matrix $\mathbf{N}$; hence the acting point is inaccurately assumed to be at point P_1 in the DR-GPI control. Moreover, the disturbance frequencies in the two simulations are the first and second eigenfrequencies of the smart beam, respectively, which are applied in the fictitious disturbance model of GPI (DR) observer. Results of the two simulations are displayed in Figures 5 and 6, which contain the sensor output voltages,

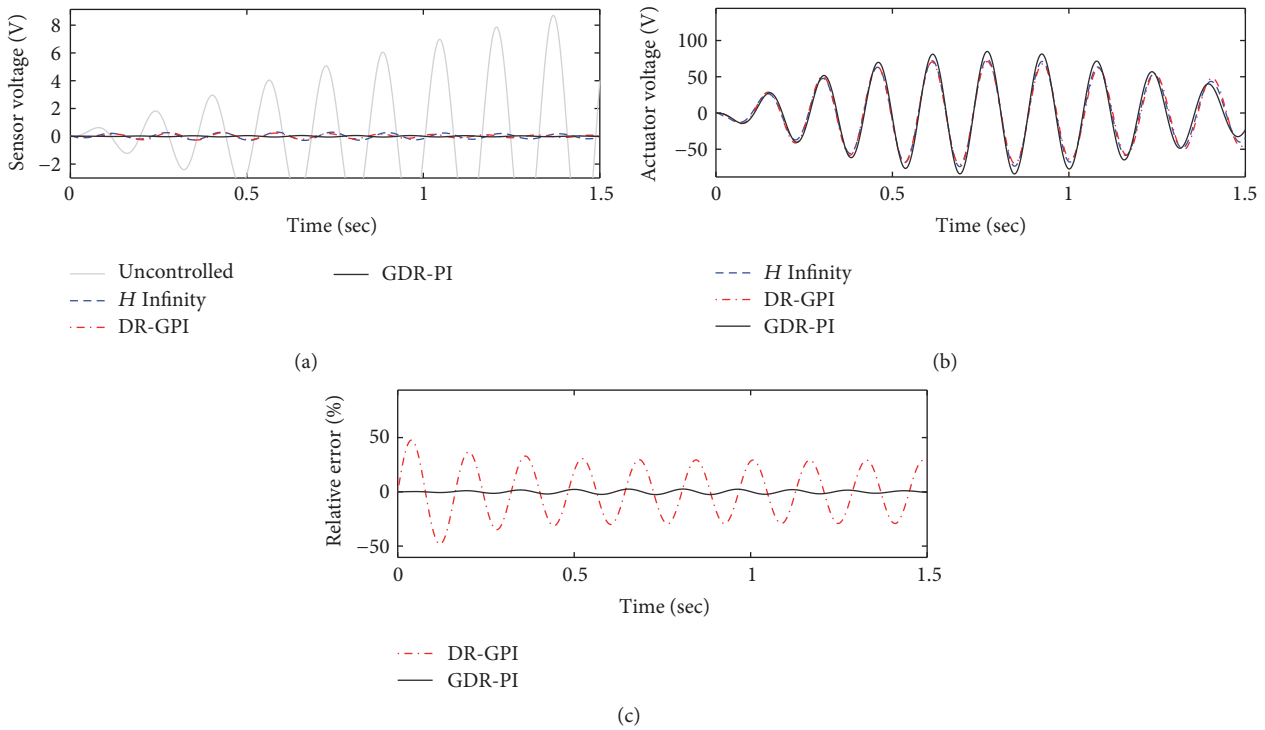

FIGURE 5: The time domain response of the controlled and uncontrolled smart beam under a harmonic disturbance with unknown influence matrix and the first eigenfrequency: (a) sensor output, (b) control input, and (c) relative error of estimated disturbance.

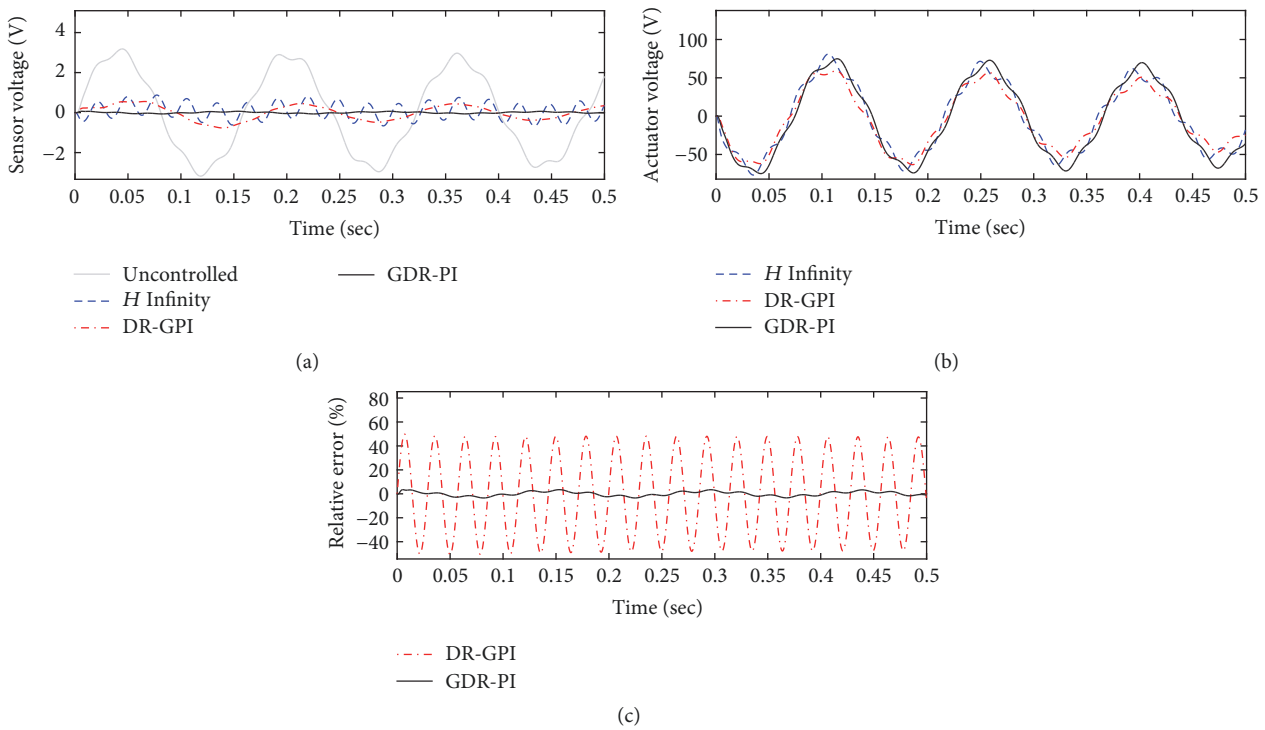

FIGURE 6: The time domain response of the controlled and uncontrolled smart beam under a harmonic disturbance with unknown influence matrix and the second eigenfrequency: (a) sensor output, (b) control input, and (c) relative error of estimated disturbance.

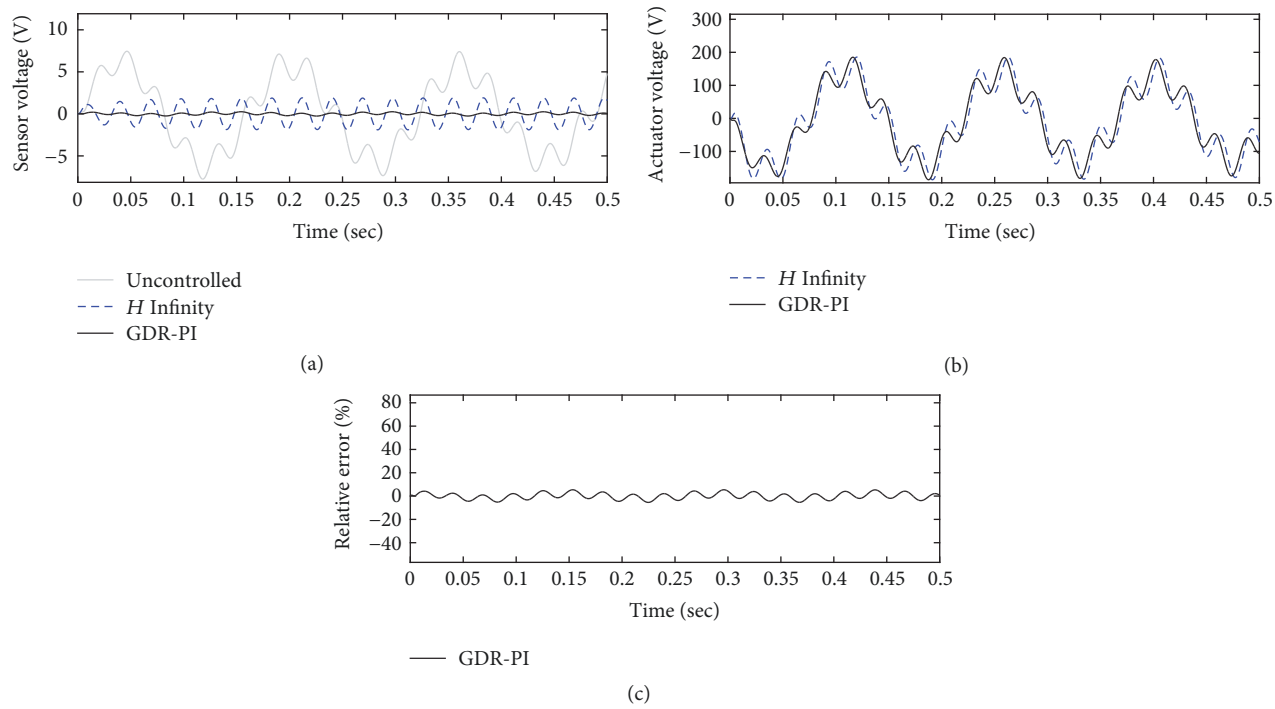

Figure 7: The time domain response of the controlled and uncontrolled smart beam under two harmonic disturbance with the second eigenfrequency applied at P_1 and P_3: (a) sensor output, (b) control input, and (c) relative error of estimated disturbance.

corresponding control voltages and relative errors of estimated disturbances and generalized disturbances. Since the tracking signals of GPI (DR) and PI (GDR) observers are different, the estimation errors of these two observers are compared through relative error, which is defined as the ratio of the difference between the real signal and the estimated signal to the peak value of the real signal. The relative errors of GPI (DR) and PI (GDR) observers in the following simulations, considering only one disturbance force and one generalized disturbance, are calculated by

$$\mathbf{r}_f = \frac{\mathbf{f} - \hat{\mathbf{f}}}{\bar{\mathbf{f}}} \times 100\%, \qquad \mathbf{r}_{fg} = \frac{\mathbf{f}_g - \mathbf{H}\hat{\mathbf{v}}}{\bar{\mathbf{f}}_\mathbf{g}} \times 100\%, \tag{62}$$

where $\mathbf{r}_f$, $\mathbf{r}_{fg}$, $\hat{\mathbf{f}}$, $\bar{\mathbf{f}}$, and $\bar{\mathbf{f}}_\mathbf{g}$ are the relative error of GPI (DR) observer, the relative error of PI (GDR) observer, the estimated disturbance force, the peak value of the disturbance force, and the peak value of the generalized disturbance, respectively. It can be seen from Figures 5(a) and 6(a) that vibrations are suppressed by all controllers and the best result is achieved by the GDR-PI control in both simulations. Due to the wrong disturbance influence matrix, the GPI (DR) observer can not estimate or counteract the disturbance accurately, which leads to decrease of vibration suppression performance. Moreover, the smart beam is exited to vibrate in the first two modals in the second simulation, whereas only the second-order modal vibration is well suppressed by the DR-GPI control, as shown in Figure 6(a). The GDR-PI control, by contrast, suppresses vibrations in two modals very well because the PI (GDR) observer does not depend on accurate influence matrix or frequency information of disturbances.

4.3.2. Multiple Disturbances with Inadequate Sensors. Secondly, H_∞ control and GDR-PI control are implemented and compared through a simulation in which two disturbance forces with the second eigenfrequency are applied at points P_1 and P_3 of the smart beam. The reason why DR-GPI control is absent is that the GPI (DR) observer requires the number of sensor signals to be no less than the number of disturbance signals, which is not satisfied in this simulation. As shown in Figures 7(a) and 7(b), even though there are two disturbance forces with high-order frequency applied, the two control methods still suppress the vibration successfully. However, the H_∞ control only achieves good suppression performance for the first-order modal vibration. Compared to the H_∞ control, the GDR-PI control achieves better vibration suppression with similar actuator voltage level for the first two modals.

4.3.3. Disturbance with Unknown Frequency. Thirdly, the disturbance influence matrices are known but the frequencies of harmonic disturbance forces are assumed to be unknown in the next two simulations. Since the GPI (DR) observer cannot work without setting the frequency of fictitious disturbance model, a wrong frequency 1 rad/s is utilized in the GPI (DR) observer. In each simulation, there is one periodic

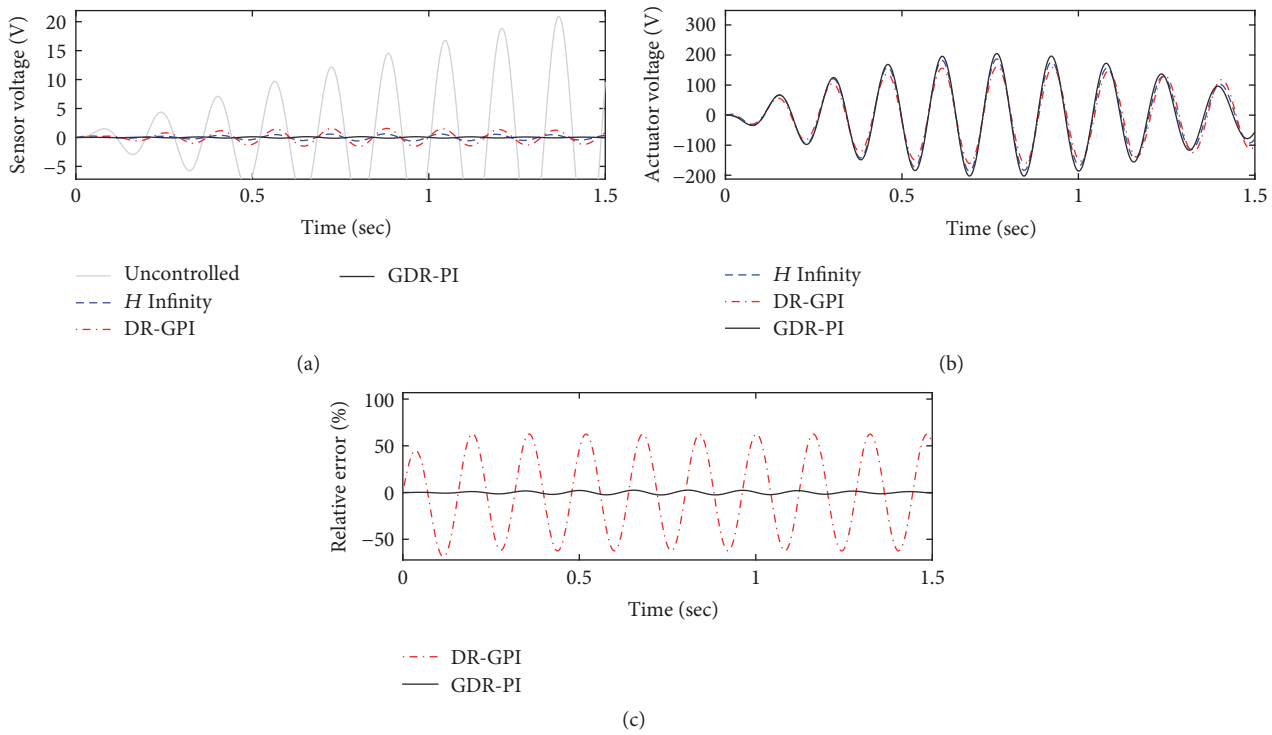

FIGURE 8: The time domain response of the controlled and uncontrolled smart beam under a harmonic disturbance with the first eigenfrequency (assumed as unknown): (a) sensor output, (b) control input, and (c) relative error of estimated disturbance.

disturbance force applied at point P_1 of the smart beam. The disturbance frequencies in the following two simulations are the first and the second eigenfrequency, respectively. The simulation results including uncontrolled and controlled vibrations, corresponding control voltages, and relative errors of estimations are shown in Figures 8 and 9. It is obvious that the GDR-PI control gives the best vibration suppression results in both simulations. As shown in Figures 8(c) and 9(c), due to lack of accurate disturbance frequency information, the estimated disturbance signal cannot converge to the real one in the GPI (DR) observer. Therefore the vibration suppression performance of DR-GPI control declines and gets even worse than the H_∞ control. On the other hand, the estimation error of the PI (GDR) observer is much smaller, which leads to better disturbance counteraction and vibration suppression, as shown in Figures 8(a) and 9(a). Interestingly, for the PI (GDR) observer, the relative estimation error of second eigenfrequency disturbance is greater than the first one, which is mainly because the estimation error caused by phase lag is more serious when the disturbance frequency gets higher.

4.3.4. Disturbance Varying Randomly. Lastly, a harmonic disturbance signal with an angular frequency varying randomly between 5 rad/s and 50 rad/s is applied at point P_1 of the smart beam in the simulation to verify and compare the three control methods. Since the randomly varying frequency can not be modeled in the GPI (DR) observer, the frequency of fictitious disturbance model of GPI (DR) observer is wrongly set as 1 rad/s. The results of uncontrolled and controlled vibrations, corresponding control voltages, and relative errors of estimations are shown in Figure 10, from which it can be found that the GDR-PI control shows obvious advantage over the other two control methods on suppressing vibrations caused by random disturbances with fast varying frequencies. Obviously, the PI (GDR) observer estimates a signal with randomly varying frequency more precisely than the GPI (DR) observer does, as shown in Figure 8(c), which leads to better vibration suppression performance. It also can be seen that the DR-GPI control performs even worse than the H_∞ control due to feeding back inaccurate estimated disturbance.

5. Conclusion

In this paper, a GDR control with PI observer has been proposed and developed for vibration suppression of piezoelectric laminated flexible smart structures under specific situations such as, but not limited to, the following: (i) known disturbance influence matrices are not available; (ii) the number of sensor signals is less than the number of disturbances; (iii) periodic disturbances with unknown high-order frequencies or random disturbances varying fast are considered. Firstly a refined state space model has been constructed; meanwhile, a generalized disturbance which includes physical disturbances and coupled state variables has been defined. Based on the refined state space model, the PI observer and GDR controller have been developed to estimate generalized disturbances and feed them back to the system, by which the physical disturbances are counteracted indirectly. Furthermore, the relationships between gain parameters and the

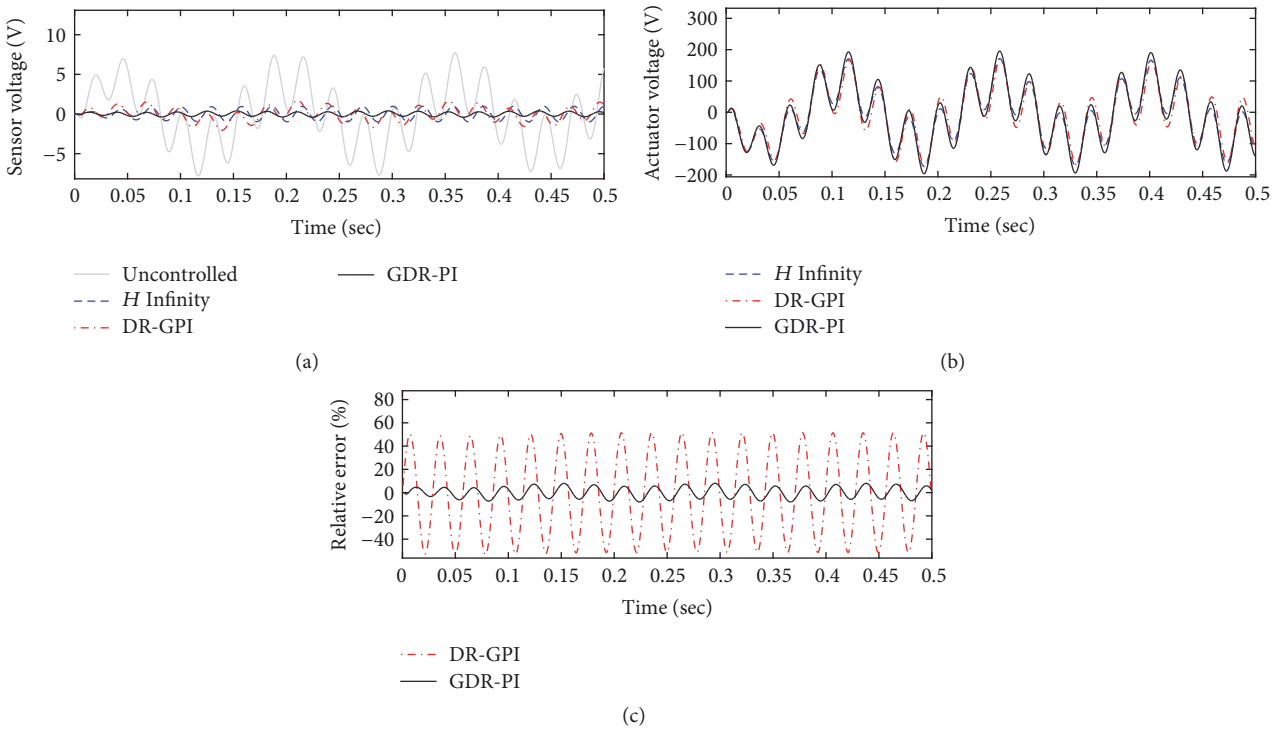

Figure 9: The time domain response of the controlled and uncontrolled smart beam under a harmonic disturbance with the second eigenfrequency (assumed as unknown): (a) sensor output, (b) control input, and (c) relative error of estimated disturbance.

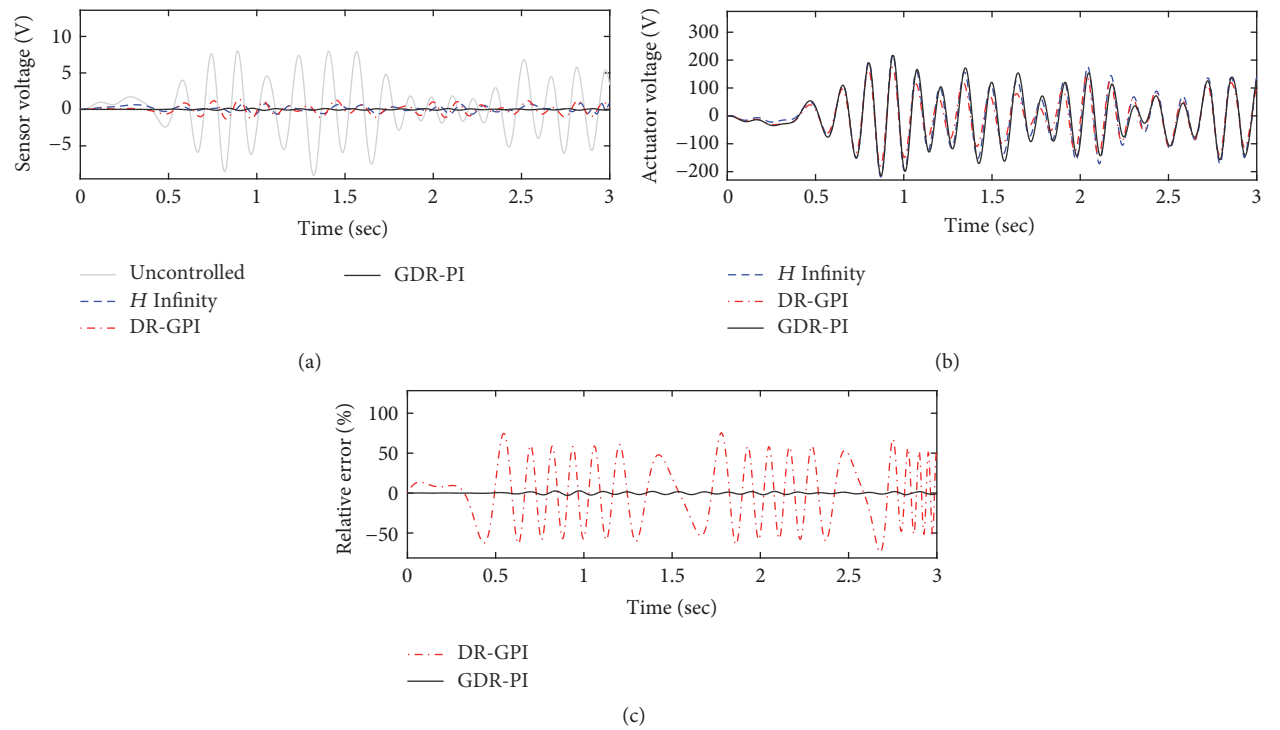

Figure 10: The time domain response of the controlled and uncontrolled smart beam under a harmonic disturbance with a randomly varying frequency: (a) sensor output, (b) control input, and (c) relative error of estimated disturbance.

performances of the PI (GDR) observer as well as the closed-loop system of GDR-PI control have been investigated.

Through the disturbance estimation and Bode diagram of PI (DR), GPI (DR), and PI (GDR) observers, it is proved that the observer gain parameter is significantly correlated with the response speed of PI (GDR) observer, and the PI (GDR) observer has better disturbance tracking capability than the other two observers. From the frequency responses of PD controller and GDR-PI controller, the controller and observer gain parameters are found out to be evidently correlated with the closed-loop system performance, especially the observer gain parameter, which means feeding back accurately estimated generalized disturbances can significantly improve the system performance. Lastly, the GDR-PI control has been validated and compared with H_∞ state feedback control and DR-GPI control, by simulations in which a piezoelectric laminated flexible smart beam is excited. The simulation results illustrate that better vibration suppression performance is obtained by the GDR-PI control under the specific situations mentioned above.

Conflicts of Interest

The authors declare that they have no conflicts of interest regarding the publication of this article.

Acknowledgments

This work is partially supported by the National Natural Science Foundation of China (nos. 51505380, 51475373, 51375390, and 11602193), Shaanxi Science and Technology Innovation Project (Grant no. 2016KTZDGY06-01), the Opening Fund of State Key Laboratory of Mechanics and Control of Mechanical Structures, Nanjing University of Aeronautics and Astronautics, China (Grant no. MCMS-0517G01), and the "111 Project" of China (no. B13044).

References

[1] Z. Wang, X. Qin, and H. T. Y. Yang, "Active suppression of panel flutter with piezoelectric actuators using eigenvector orientation method," *Journal of Sound and Vibration*, vol. 331, no. 7, pp. 1469–1482, 2012.

[2] J. Dosch, D. Leo, and D. Inman, "Modeling and control for vibration suppression of a flexible active structure," *Journal of Guidance, Control, and Dynamics*, vol. 18, no. 2, pp. 340–346, 1995.

[3] M. Sabatini, P. Gasbarri, R. Monti, and G. B. Palmerini, "Vibration control of a flexible space manipulator during on orbit operations," *Acta Astronautica*, vol. 73, pp. 109–121, 2012.

[4] V. Balamurugan and S. Narayanan, "Shell finite element for smart piezoelectric composite plate/shell structures and its application to the study of active vibration control," *Finite Elements in Analysis and Design*, vol. 37, no. 9, pp. 713–718, 2001.

[5] X. Q. He, T. Y. Ng, S. Sivashanker, and K. M. Liew, "Active control of FGM plates with integrated piezoelectric sensors and actuators," *International Journal of Solids and Structures*, vol. 38, no. 9, pp. 1641–1655, 2001.

[6] Y. K. Kang, H. C. Park, J. Kim, and S.-B. Choi, "Interaction of active and passive vibration control of laminated composite beams with piezoceramic sensors/actuators," *Materials and Corrosion*, vol. 23, no. 3, pp. 277–286, 2002.

[7] K. M. Liew, X. Q. He, T. Y. Ng, and S. Sivashanker, "Active control of FGM plates subjected to a temperature gradient: Modelling via finite element method based on FSDT," *International Journal for Numerical Methods in Engineering*, vol. 52, no. 11, pp. 1253–1271, 2001.

[8] J. M. S. Moita, I. F. P. Correia, C. M. M. Soares, and C. A. M. Soares, "Active control of adaptive laminated structures with bonded piezoelectric sensors and actuators," *Computers & Structures*, vol. 82, no. 17–19, pp. 1349–1358, 2004.

[9] S. Y. Wang, S. T. Quek, and K. K. Ang, "Vibration control of smart piezoelectric composite plates," *Smart Materials and Structures*, vol. 10, no. 4, pp. 637–644, 2001.

[10] J. J. Dosch, D. J. Inman, and E. Garcia, "Self-sensing piezoelectric actuator for collocated control," *Journal of Intelligent Material Systems and Structures*, vol. 3, no. 1, pp. 166–185, 1992.

[11] M. K. Kwak and S. Heo, "Active vibration control of smart grid structure by multiinput and multioutput positive position feedback controller," *Journal of Sound and Vibration*, vol. 304, no. 1-2, pp. 230–245, 2007.

[12] J. Shan, H. T. Liu, and D. Sun, "Slewing and vibration control of a single-link flexible manipulator by positive position feedback (PPF)," *Mechatronics*, vol. 15, no. 4, pp. 487–503, 2005.

[13] G. Song, S. P. Schmidt, and B. N. Agrawal, "Experimental robustness study of positive position feedback control for active vibration suppression," *Journal of Guidance, Control, and Dynamics*, vol. 25, no. 1, pp. 179–182, 2002.

[14] E. Omidi and S. N. Mahmoodi, "Vibration control of collocated smart structures using H ∞ modified positive position and velocity feedback," *Journal of Vibration and Control*, vol. 22, no. 10, pp. 2434–2442, 2016.

[15] H. Karagülle, L. Malgaca, and H. F. Öktem, "Analysis of active vibration control in smart structures by ANSYS," *Smart Materials and Structures*, vol. 13, no. 4, pp. 661–667, 2004.

[16] S. M. Khot, N. P. Yelve, R. Tomar, S. Desai, and S. Vittal, "Active vibration control of cantilever beam by using PID based output feedback controller," *Journal of Vibration and Control*, vol. 18, no. 3, pp. 366–372, 2012.

[17] S.-Q. Zhang, Y.-X. Li, and R. Schmidt, "Active shape and vibration control for piezoelectric bonded composite structures using various geometric nonlinearities," *Composite Structures*, vol. 122, pp. 239–249, 2015.

[18] J. Fei, "Active vibration control of flexible steel cantilever beam using piezoelectric actuators," in *Proceedings of the 37th Southeastern Symposium on System Theory (SST '05)*, pp. 35–39, IEEE, March 2004.

[19] Y. Shen and A. Homaifar, "Vibration control of flexible structures with PZT sensors and actuators," *Journal of Vibration and Control*, vol. 7, no. 3, pp. 417–451, 2001.

[20] J. C. Bruch Jr., J. M. Sloss, S. Adali, and I. S. Sadek, "Modified bang-bang piezoelectric control of vibrating beams," *Smart Materials and Structures*, vol. 8, no. 5, pp. 647–653, 1999.

[21] K. Makihara, J. Onoda, and K. Minesugi, "Using tuned electrical resonance to enhance bang-bang vibration control," *AIAA Journal*, vol. 45, no. 2, pp. 497–504, 2007.

[22] H. S. Tzou and W. K. Chai, "Design and testing of a hybrid polymeric electrostrictive/piezoelectric beam with bang-bang control," *Mechanical Systems and Signal Processing*, vol. 21, no. 1, pp. 417–429, 2007.

[23] Y. Wang and D. J. Inman, "Comparison of control laws for vibration suppression based on energy consumption," *Journal of Intelligent Material Systems and Structures*, vol. 22, no. 8, pp. 795–809, 2011.

[24] S. Narayanan and V. Balamurugan, "Finite element modelling of piezolaminated smart structures for active vibration control with distributed sensors and actuators," *Journal of Sound and Vibration*, vol. 262, no. 3, pp. 529–562, 2003.

[25] E. Padoin, O. Menuzzi, E. A. Perondi, and J. S. O. Fonseca, "Modeling and LQR/LQG control of a cantilever beam using piezoelectric material in," in *Proceedings of the 22nd International Congress of Mechanical EngineeringCOBEM*, vol. 2013, 2013.

[26] C. M. A. Vasques and J. Dias Rodrigues, "Active vibration control of smart piezoelectric beams: comparison of classical and optimal feedback control strategies," *Computers & Structures*, vol. 84, no. 22-23, pp. 1402–1414, 2006.

[27] K. R. Kumar and S. Narayanan, "Active vibration control of beams with optimal placement of piezoelectric sensor/actuator pairs," *Smart Materials and Structures*, vol. 17, no. 5, Article ID 055008, 2008.

[28] J.-H. Man, K.-H. Rew, and I. Lee, "An experimental study of active vibration control of composite structures with a piezoceramic actuator and a piezo-film sensor," *Smart Materials and Structures*, vol. 6, no. 5, pp. 549–558, 1997.

[29] W. P. Li and H. Huang, "Integrated optimization of actuator placement and vibration control for piezoelectric adaptive trusses," *Journal of Sound and Vibration*, vol. 332, no. 1, pp. 17–32, 2013.

[30] J. W. Sohn, S.-B. Choi, and H. S. Kim, "Vibration control of smart hull structure with optimally placed piezoelectric composite actuators," *International Journal of Mechanical Sciences*, vol. 53, no. 8, pp. 647–659, 2011.

[31] Z.-G. Song and F.-M. Li, "Optimal locations of piezoelectric actuators and sensors for supersonic flutter control of composite laminated panels," *Journal of Vibration and Control*, vol. 20, no. 14, pp. 2118–2132, 2013.

[32] Y. H. Zhao and H. Y. Hu, "Active control of vertical tail buffeting by piezoelectric actuators," *Journal of Aircraft*, vol. 46, no. 4, pp. 1167–1175, 2009.

[33] S. Kapuria and M. Yaqoob Yasin, "Active vibration control of piezoelectric laminated beams with electroded actuators and sensors using an efficient finite element involving an electric node," *Smart Materials and Structures*, vol. 19, no. 4, Article ID 045019, 2010.

[34] R. Lammering, "The application of a finite shell element for composites containing piezo-electric polymers in vibration control," *Computers & Structures*, vol. 41, no. 5, pp. 1101–1109, 1991.

[35] H. S. Tzou and C. I. Tseng, "Distributed modal identification and vibration control of continua. Piezoelectric finite element formulation and analysis," *Journal of Dynamic Systems, Measurement, and Control*, vol. 113, no. 3, pp. 500–505, 1991.

[36] M. Dadfarnia, N. Jalili, B. Xian, and D. M. Dawson, "A lyapunov-based piezoelectric controller for flexible cartesian robot manipulators," *Journal of Dynamic Systems, Measurement, and Control*, vol. 126, no. 2, pp. 347–358, 2004.

[37] S. B. Choi and J. W. Sohn, "Chattering alleviation in vibration control of smart beam structures using piezofilm actuators: Experimental verification," *Journal of Sound and Vibration*, vol. 294, no. 3, pp. 640–649, 2006.

[38] Z.-C. Qiu, J.-D. Han, X.-M. Zhang, Y.-C. Wang, and Z.-W. Wu, "Active vibration control of a flexible beam using a noncollocated acceleration sensor and piezoelectric patch actuator," *Journal of Sound and Vibration*, vol. 326, no. 3–5, pp. 438–455, 2009.

[39] M.-H. Kim and D. J. Inman, "Reduction of observation spillover in vibration suppression using a sliding mode observer," *Journal of Vibration and Control*, vol. 7, no. 7, pp. 1087–1105, 2001.

[40] J. Richelot, J. B. Guibe, and V. P. Budinger, "Active control of a clamped beam equipped with piezoelectric actuator and sensor using generalized predictive control," in *Proceedings of the IEEE International Symposium on Industrial Electronics (ISlE '04)*, vol. 1, pp. 583–588, May 2004.

[41] A. G. Wills, D. Bates, A. J. Fleming, B. Ninness, and S. O. R. Moheimani, "Model predictive control applied to constraint handling in active noise and vibration control," *IEEE Transactions on Control Systems Technology*, vol. 16, no. 1, pp. 3–12, 2008.

[42] R. Dubay, M. Hassan, C. Li, and M. Charest, "Finite element based model predictive control for active vibration suppression of a one-link flexible manipulator," *ISA Transactions*, vol. 53, no. 5, pp. 1609–1619, 2014.

[43] G. L. C. M. De Abreu and J. F. Ribeiro, "A self-organizing fuzzy logic controller for the active control of flexible structures using piezoelectric actuators," *Applied Soft Computing*, vol. 1, no. 4, pp. 271–283, 2002.

[44] M. Marinaki, Y. Marinakis, and G. E. Stavroulakis, "Fuzzy control optimized by a Multi-Objective Differential Evolution algorithm for vibration suppression of smart structures," *Computers & Structures*, vol. 147, pp. 126–137, 2015.

[45] J.-J. Wei, Z.-C. Qiu, Y.-C. Wang, and J.-D. Han, "Experimental comparison research on active vibration control for flexible piezoelectric manipulator using fuzzy controller," *Journal of Intelligent & Robotic Systems*, vol. 59, no. 1, pp. 31–56, 2010.

[46] O. Abdeljaber, O. Avci, and D. J. Inman, "Active vibration control of flexible cantilever plates using piezoelectric materials and artificial neural networks," *Journal of Sound and Vibration*, vol. 363, pp. 33–53, 2016.

[47] M. T. Valoor, K. Chandrashekhara, and S. Agarwal, "Self-adaptive vibration control of smart composite beams using recurrent neural architecture," *International Journal of Solids and Structures*, vol. 38, no. 44-45, pp. 7857–7874, 2001.

[48] C. P. Smyser and K. Chandrashekhara, "Robust vibration control of composite beams using piezoelectric devices and neural networks," *Smart Materials and Structures*, vol. 6, no. 2, pp. 178–189, 1997.

[49] R. Kumar, S. P. Singh, and H. N. Chandrawat, "MIMO adaptive vibration control of smart structures with quickly varying parameters: Neural networks vs classical control approach," *Journal of Sound and Vibration*, vol. 307, no. 3-5, pp. 639–661, 2007.

[50] Z. Qiu, X. Zhang, and C. Ye, "Vibration suppression of a flexible piezoelectric beam using BP neural network controller," *Acta Mechanica Solida Sinica*, vol. 25, no. 4, pp. 417–428, 2012.

[51] R. Jha and J. Rower, "Experimental investigation of active vibration control using neural networks and piezoelectric actuators," *Smart Materials and Structures*, vol. 11, no. 1, pp. 115–121, 2002.

[52] J. Jiang and D. Li, "Optimal placement and decentralized robust vibration control for spacecraft smart solar panel structures," *Smart Materials and Structures*, vol. 19, no. 8, Article ID 085020, 2010.

[53] X. Wang, Y. Liu, W. Gao, and J. Chen, "Robust control of uncertain piezoelectric laminated plates based on model reduction," *AIAA Journal*, vol. 49, no. 11, pp. 2337–2348, 2011.

[54] S. M. Hasheminejad, M. Vahedi, and A. H. D. Markazi, "Multi-objective robust active vibration control of an arbitrary thick piezolaminated beam," *Mechanics of Advanced Materials and Structures*, vol. 22, no. 11, pp. 908–924, 2015.

[55] I. D. Landau, A. Castellanos Silva, T.-B. Airimitoaie, G. Buche, and M. Noë, "Benchmark on adaptive regulation—rejection of unknown/time-varying multiple narrow band disturbances," *European Journal of Control*, vol. 19, no. 4, pp. 237–252, 2013.

[56] X. Chen and M. Tomizuka, "A minimum parameter adaptive approach for rejecting multiple narrow-band disturbances with application to hard disk drives," *IEEE Transactions on Control Systems Technology*, vol. 20, no. 2, pp. 408–415, 2012.

[57] S. Aranovskiy and L. B. Freidovich, "Adaptive compensation of disturbances formed as sums of sinusoidal signals with application to an active vibration control benchmark," *European Journal of Control*, vol. 19, no. 4, pp. 253–265, 2013.

[58] W. He and S. S. Ge, "Robust adaptive boundary control of a vibrating string under unknown time-varying disturbance," *IEEE Transactions on Control Systems Technology*, vol. 20, no. 1, pp. 48–58, 2012.

[59] J. Q. Han, "From PID to active disturbance rejection control," *IEEE Transactions on Industrial Electronics*, vol. 56, no. 3, pp. 900–906, 2009.

[60] Z. Gao, "Scaling and bandwidth-parameterization based controller tuning," in *Proceedings of the American Control Conference*, pp. 4989–4996, Denver, Colo, USA, June 2003.

[61] S. Li, J. Li, and Y. Mo, "Piezoelectric multimode vibration control for stiffened plate using ADRC-based acceleration compensation," *IEEE Transactions on Industrial Electronics*, vol. 61, no. 12, pp. 6892–6902, 2014.

[62] S. Li, J. Li, Y. Mo, and R. Zhao, "Composite multi-modal vibration control for a stiffened plate using non-collocated acceleration sensor and piezoelectric actuator," *Smart Materials and Structures*, vol. 23, no. 1, Article ID 015006, 2014.

[63] P. C. Müller and J. Lückel, "Optimal multivariable feedback system design with disturbance rejection," *Problems of Control and Information Theory*, vol. 6, no. 3, pp. 211–227, 1977.

[64] S. Q. Zhang, H. N. Li, R. Schmidt, and P. C. Müller, "Disturbance rejection control for vibration suppression of piezoelectric laminated thin-walled structures," *Journal of Sound and Vibration*, vol. 333, no. 5, pp. 1209–1223, 2014.

[65] S.-Q. Zhang, R. Schmidt, P. C. Müller, and X.-S. Qin, "Disturbance rejection control for vibration suppression of smart beams and plates under a high frequency excitation," *Journal of Sound and Vibration*, vol. 353, pp. 19–37, 2015.

[66] S. Q. Zhang and R. Schmidt, "Large rotation FE transient analysis of piezolaminated thin-walled smart structures," *Smart Materials and Structures*, vol. 22, no. 10, Article ID 105025, 2013.

[67] S.-Q. Zhang, Y.-X. Li, and R. Schmidt, "Modeling and simulation of macro-fiber composite layered smart structures," *Composite Structures*, vol. 126, pp. 89–100, 2015.

[68] S. Q. Zhang and R. Schmidt, "Static and dynamic FE analysis of piezoelectric integrated thin-walled composite structures with large rotations," *Composite Structures*, vol. 112, no. 1, pp. 345–357, 2014.

[69] S. Zhang, R. Schmidt, and X. Qin, "Active vibration control of piezoelectric bonded smart structures using PID algorithm," *Chinese Journal of Aeronautics*, vol. 28, no. 1, pp. 305–313, 2015.

[70] P. C. Müller, "Design of PI-observers and compensators for nonlinear control system," *Advances in Mechanics, Dynamics and Control*, pp. 223–231, 2008.

[71] W. S. Levine, Ed., *Control System Fundamentals*, CRC Press, Boca Raton, Fla, USA, 2000.